

NJC

Accepted Manuscript



This is an *Accepted Manuscript*, which has been through the Royal Society of Chemistry peer review process and has been accepted for publication.

Accepted Manuscripts are published online shortly after acceptance, before technical editing, formatting and proof reading. Using this free service, authors can make their results available to the community, in citable form, before we publish the edited article. We will replace this *Accepted Manuscript* with the edited and formatted *Advance Article* as soon as it is available.

You can find more information about *Accepted Manuscripts* in the [Information for Authors](#).

Please note that technical editing may introduce minor changes to the text and/or graphics, which may alter content. The journal's standard [Terms & Conditions](#) and the [Ethical guidelines](#) still apply. In no event shall the Royal Society of Chemistry be held responsible for any errors or omissions in this *Accepted Manuscript* or any consequences arising from the use of any information it contains.

Hierarchical ZSM-5 zeolite with uniform mesopores and improved catalytic properties

D. P. Serrano^{1,2,*}, J. M. Escola², R. Sanz², R.A. Garcia², A. Peral², I. Moreno² and M. Linares²

¹IMDEA Energy Institute, Avda Ramón de la Sagra, nº 3, 28935, Móstoles (Spain)

²Environmental and Chemical Engineering Group, ESCET, Rey Juan Carlos University, c/

Tulipán s/n, 28933, Móstoles (Spain)

* to whom correspondence should be addressed

e-mail: david.serrano@urjc.es

Tel: +34 91 488 74 50; Fax: +34 91 488 70 68

Abstract

Hierarchical ZSM-5 with uniform mesoporosity has been here synthesized through the sequential coupling of two strategies: generation of a secondary porosity by crystallization of silanized protozeolitic units and subsequent treatment with a basic surfactant-containing solution. The ZSM-5 zeolite so obtained exhibits a high crystallinity and contains two levels of uniform porosities within the micro- and mesopore ranges, respectively. The uniform mesoporosity is the result of the reorganization of irregular mesopores, created initially from the silanized protozeolitic units, by means of the local rearrangement of zeolitic fragments, promoted by the contact with a cationic surfactant under mild basic conditions. Interestingly, this second treatment is little effective when it is applied to a non-hierarchical ZSM-5 sample, denoting that the presence of an initial secondary porosity is essential for affording the surfactant/ammonia solution to modify the zeolite and, consequently, for the formation of uniform mesopores. Characterization of the zeolite samples by means of different techniques pointed out that the crystallinity, Al coordination and the acidic features of the zeolite do not change meaningfully after the mesopore narrowing treatment, although significant variations in the textural properties are observed as it was expected. The effects of the occurrence of a regular mesoporosity on the catalytic properties of the hierarchical ZSM-5 zeolite were proved using the acylation of 2-methoxynaphthalene as test reaction. The material having uniform mesopores showed both the highest activity and selectivity towards 6-acetyl-2-methoxynaphthalene, which was interpreted as a result of the presence of a more regular and less rough mesopore surface, which in turn facilitates the interaction between the reactant molecules and the active sites located and distributed over the mesopores.

Keywords: hierarchical ZSM-5; protozeolitic unit silanization; surfactant-mediated reorganization; uniform mesoporosity.

1. INTRODUCTION

The preparation of hierarchical zeolites has been a booming research field along the last decade¹⁻¹¹. Hierarchical zeolites are characterized by the presence of a bimodal porous distribution, having a combination of micro- and mesopores. The occurrence of mesoporosity allows the reagents to have a better accessibility towards the active sites, removing steric limitations and shortening additionally the intracrystalline diffusion pathways¹². These features have resulted in several advantages such as enhanced activities¹³, better dispersion of metal active phases^{14,15} and lower deactivation rates¹⁶. Different procedures have been proposed for the preparation of hierarchical zeolites, such as dealumination¹⁷, carbon templating¹¹, desilication¹⁸, protozeolitic units silanization^{6,9,10}, use of amphiphile organosilanes⁷ and dual templating with surfactants⁸. Although these methods enable to obtain hierarchical zeolites, the nature of the attained mesoporosity differs meaningfully among them since the underlying principles of the different procedures are very diverse. Thus, the BET surface area values exhibited by hierarchical zeolites prepared by the protozeolitic units silanization and desilication methods were distinctly higher than those of the hierarchical zeolites obtained by the carbon templating route^{11,12}. Moreover, the contribution and properties of the mesoporosity so generated are difficult to be adjusted, usually showing a wide pore size distribution. The importance of mesopore quality and pore connectivity in the enhanced catalyst lifetime of hierarchical zeolites has been recently highlighted^{19,20}. In this way, a high contribution of the hierarchical porosity and mesopore connectivity has been recently achieved from disordered MFI nanosheets with 2.5 nm thickness, giving rise to increased conversion in the Pechmann condensation of pyrogallol and resorcinol²¹.

One successful approach affording hierarchical zeolites is the method based on the crystallization of protozeolitic units, previously functionalized with organosilanes, which prevents partially their aggregation into conventional zeolite crystals. After calcination, the space

previously occupied by the organosilane is released, giving rise to the appearance of supermicro- and mesopores. This method has shown generality since it has been applied successfully to a variety of zeolites such as ZSM-5, TS-1, Beta or mordenite¹. Additionally, the amount and nature of the organosilane is a key element for tailoring the attained mesoporosity^{22–25}. However, as in other strategies, the hierarchical zeolites so obtained usually present a broad mesopore distribution, encompassing the 2 - 8 nm range. Other silanization-based methods, which employ silylated polymers as organosilanes, also share this drawback and lead to hierarchical zeolites with non-uniform mesopores⁶. The use of amphiphile organosilanes has afforded the preparation of hierarchical zeolites with narrower pore size distributions⁷, although in some cases it has been detected the presence of a portion of the initial amorphous phase, not completely dissolved and converted, in the final zeolitic material^{26,27}.

Desilication is other treatment extensively investigated for developing zeolitic materials with mesoporosity. This method follows a really simple approach consisting of treating the zeolite in a strong alkaline medium under controlled conditions, which causes the extraction and removal of a part of the silica from the zeolite framework. Consequently, significant variations are observed between the Si/Al ratio of the raw zeolite and the final hierarchical one. The desilication route has proved to be a versatile procedure capable of leading to the synthesis of different mesoporous zeolites^{18,28}, although having usually broad mesopore size distributions. Moreover, this route is strongly dependent on the Si/Al atomic ratio of the starting zeolite¹⁸ and often requires the use of different treatments, such as acid washing or the addition of tetraalkylammonium cations (e.g. TPAOH) to the alkaline solution, which act as “pore growth moderators”²⁹. A remarkable result has been obtained by the group of Fajula when applying the desilication method to USY zeolites previously dealuminated, which has led to the development of hierarchical zeolites with trimodal porosity³⁰.

Other interesting alternative for the preparation of hierarchical zeolites is the one based on the treatment of the zeolite with a surfactant-containing alkaline solution³¹⁻³². The alkaline medium is provided by an ammonia solution, having a mild basicity, which seems to be an important aspect to avoid the occurrence of desilication phenomena. Garcia-Martínez et al.³¹ has proved that this treatment is very effective when applied to dealuminated zeolite Y, showing the generation of uniform mesopores as a result of the treatment with the surfactant/ammonia solution. This important finding has been later confirmed by other researchers following a similar procedure³².

In this context, the present work reports the preparation of hierarchical ZSM-5 following a route that has been envisaged as the sequential combination of two of the approaches above described. Firstly, a secondary porosity is induced in the zeolite by crystallization of silanized protozeolitic nanounits. The irregular mesopores so obtained are then reorganized by treatment with a surfactant-containing alkaline solution, leading to materials with a narrow mesopore size distribution. The results here reported prove the need of the existence of a previous amount of mesoporosity as an essential aspect for the surfactant reorganization treatment to be effective. In a recent work, our group has reported the combination of these strategies for the preparation of hierarchical TS-1 zeolite with uniform mesoporosity³³, showing now that it can be successfully applied for ZSM-5 zeolite. Additionally, in the present work a general mechanism is proposed to explain the generation of the observed uniform mesoporosity. Other relevant conclusion derived from the results here reported is the observation that narrowing the mesopore size distribution induces significant improvements in the catalytic properties exhibited by the hierarchical ZSM-5 in the acylation of 2-methoxynaphthalene.

2. EXPERIMENTAL

2.1. Catalysts Preparation

a) Materials synthesis

Hierarchical ZSM-5 was synthesized by crystallization of silanized protozeolitic units, according to a method earlier published in the literature⁹. Initially, a precursor ZSM-5 zeolite solution was prepared with the following molar composition: 1 Al₂O₃ : 60 SiO₂ : 11 TPAOH : 1500 H₂O. Tetraethoxysilane (TEOS, 98%; Aldrich), aluminum isopropoxide (AIP; Aldrich), tetrapropylammonium hydroxide (TPAOH, 40%; Alfa), and distilled water were used as starting reagents. Firstly, the precursor solution was aged at ambient temperature for 44 h and then it was precrystallized under reflux and stirring (100 rpm) at 90 °C for 22 h. Then, the resulting zeolite protozeolitic units were functionalized with phenylaminopropyltrimethoxysilane (PHAPTMS, Aldrich). The organosilane was added in a proportion of 8 mol% with respect to the silica content in the initial gel and the silanization reaction was performed at 90 °C for 6 h. Finally, crystallization was carried out in Teflon®-lined stainless-steel autoclaves under static conditions and autogenous pressure at 170 °C for 7 days. The solid product obtained was separated by centrifugation, washed several times with distilled water, dried overnight at 110 °C and calcined in air at 550 °C for 5 h. This sample was denoted as h-ZSM-5.

For comparison purposes, conventional ZSM-5 was synthesized as reference following the same procedure above described, but omitting the precrystallization and organosilane functionalization steps. Likewise, a sample of Al-MCM-41 was prepared for catalytic comparison according to a procedure published elsewhere³⁴ from a solution with the following molar composition: Al₂O₃ : 60 SiO₂ : 9 CTABr : 165 NH₃ : 8000 H₂O.

2.2. Mesopore Narrowing Treatment

The synthesized zeolites were calcined and subsequently subjected to the mesopore narrowing treatment by contacting with a surfactant-containing ammonia solution. In this procedure, 1.00 g of calcined zeolitic material was dispersed in 62.8 g of a 0.37 M NH_4OH aqueous solution containing 0.7 g of hexadecyltrimethylammonium bromide (Aldrich). The resultant mixture was stirred at room temperature for 30 min, being then loaded into an autoclave and subjected to a hydrothermal treatment for 20 h at 150 °C. The solid obtained was recovered by centrifugation, washed several times with distilled water, dried overnight at 110 °C and, finally, calcined at 550 °C for 5 h. The samples thus prepared from the conventional and hierarchical ZSM-5 samples were denoted as ZSM-5 (mnt) and h-ZSM-5 (mnt), respectively.

2.3. Characterization of the catalysts

All samples were characterized by a number of techniques in order to determine their main physicochemical properties. Powder X-Ray Diffraction (XRD) patterns were collected employing $\text{CuK}\alpha$ radiation on a Philips X'PERT MPD diffractometer. Diffraction data were recorded in the range 5 - 50°, using a step size of 0.02° and a counting time of 10 s, respectively. The Si and Al contents of the catalysts were determined by Inductively Coupled Plasma Atomic Emission Spectroscopy (ICP-AES) using a Varian Vista AX instrument. High-resolution ^{27}Al MAS-NMR spectra of the zeolite samples were recorded at 104.1 MHz using a Varian Infinity 400 spectrometer. All the measurements were carried out at ambient temperature with a spinning frequency of 11 kHz and pulse width of 2.5 s. Transmission Electron Microscopy (TEM) images were obtained with a PHILIPS TECHNAI 20 microscope operating at 200 kV. Thereby, the samples were crushed, dispersed in acetone and deposited on a carbon-coated copper grid.

Argon adsorption-desorption isotherms were obtained using a Micromeritics ASAP 2010 instrument at -186 °C (87.5 K). The samples were evacuated at 300 °C under vacuum for 12 h

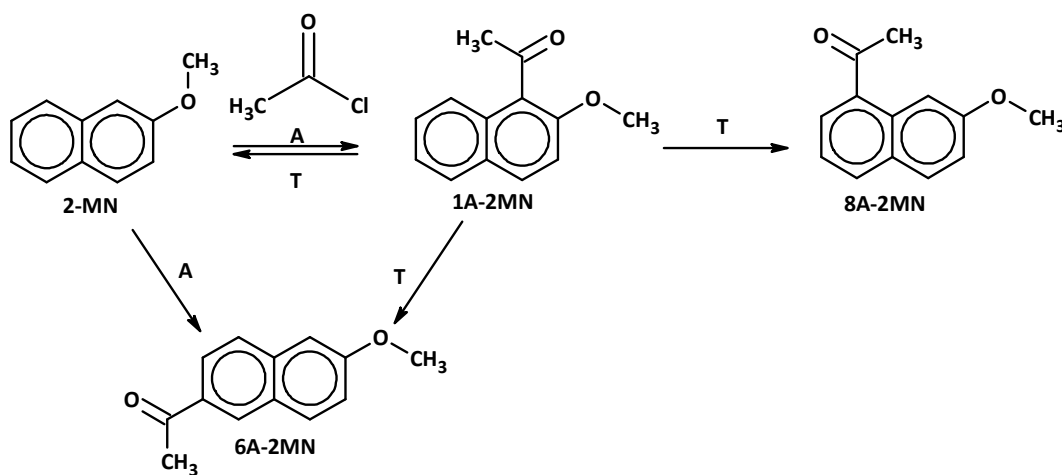
prior to the analyses. The textural properties of the synthesized materials were determined from the adsorption-desorption isotherms. Specific surface areas were calculated using the BET equation, while the cumulative pore volume curves and pore size distributions (PSD) were estimated by applying the NLDFT method to the adsorption branch of the isotherms, assuming cylindrical pore geometry. This method has been also employed for determining the relative contribution of micro- and mesopores to both surface area and pore volume.

FTIR spectra of previously adsorbed pyridine on the zeolite samples were recorded on a Jasco 6300 FTIR spectrophotometer, working with a resolution of 4 cm^{-1} . Self-supporting wafers of the zeolites with a thickness of ca. 6 mg cm^{-2} were prepared by pressing ($7 \times 10^3\text{ kg cm}^{-2}$) the powdered sample for 10 min. Before measurements, the wafers were degassed at $500\text{ }^\circ\text{C}$ for 4 h in a vacuum cell fitted with greaseless stopcocks and KBr windows under a residual pressure of $2 \times 10^{-4}\text{ mbar}$. Then, the sample temperature was decreased to $150\text{ }^\circ\text{C}$ and exposed to pyridine vapour (1.5 mbar pressure) for 5 min. The physically adsorbed pyridine fraction was removed by degassing the sample for 30 min at $150\text{ }^\circ\text{C}$. Once the spectrum was recorded, the sample was degassed again at increasing temperatures in the range $250\text{--}450\text{ }^\circ\text{C}$ while recording the spectra at each degassing temperature. For quantitative characterization of the acid sites, the following bands and absorption coefficients were used: pyridine PyH^+ band at $1543\text{--}1548\text{ cm}^{-1}$ ($\epsilon = 1.67\text{ cm } \mu\text{mol}^{-1}$) for the Brönsted acid sites and pyridine PyL bands at $1455\text{--}1446\text{ cm}^{-1}$ ($\epsilon = 2.2\text{ cm } \mu\text{mol}^{-1}$) for the Lewis acid sites³⁵.

2.4. Catalytic tests

The catalytic properties of the samples were tested in 2-methoxynaphthalene (2-MN) acylation using acetyl chloride as acylating agent (Scheme 1). The catalytic tests were carried out under atmospheric pressure in a 100-mL three-necked batch reactor equipped with a reflux condenser, a thermometer and a magnetic stirrer. In a typical reaction, 0.75 g of 2-MN in 20 mL of solvent

(nitrobenzene) was loaded into the reactor. Subsequently, 0.200 mL of sulpholane, used as internal standard, and 0.150 g of fresh catalyst (catalyst/2-MN = 0.20 w/w) were added to the reaction mixture, being kept magnetically stirred under nitrogen. Once the reaction temperature (180 °C) was reached, 0.330 mL of acylating agent (acetyl chloride) was added to the flask. Periodically, aliquots of the reaction mixture were collected in order to assess the time evolution of the reaction, the mixture being allowed to react for 180 min. The products were analyzed by capillary gas chromatography in a Varian 3900 Series instrument equipped with a 30 m x 0.25 mm capillary column (CP SIL 8 CB) and a FID detector.



Scheme 1. Acylation of 2-MN

3. RESULTS AND DISCUSSION

The present work reports a synthesis strategy for the preparation of hierarchical ZSM-5 having a narrow mesopore size distribution and how this feature affects and improves its physicochemical and catalytic properties. The method here outlined consists of the combination of two different approaches:

- The generation of a secondary porosity by the addition of a silanization agent to the zeolite precursor gel, which has been earlier demonstrated to be very effective for hindering

partially the aggregative growth of zeolitic nanounits and, therefore, leading to the appearance of super-micro and mesopores once the organic compounds are removed by calcination⁹. This secondary porosity is not uniform and shows typically a relatively broad pore size distribution.

- The capability of surfactant/ammonia solutions, under hydrothermal conditions, to promote the local rearrangement of zeolitic fragments. This effect has been recently reported by García-Martínez et al.³¹ applied to dealuminated zeolite Y. However, as it will be shown here, the effectiveness of this treatment alone is quite limited if the parent material contains solely the typical zeolitic micropores.

3.1. Changes induced in the physicochemical properties of ZSM-5 zeolite

The first experiments were designed to establish whether the secondary porosity generated by the protozeolitic silanization route might be turned into a uniform mesoporosity using a mesopore narrowing treatment consisting of the addition of a solution containing ammonia plus the surfactant (hexadecyltrimethylammonium bromide). Additionally, another point of interest was to ascertain whether the presence of this initial mesoporosity is an essential aspect to promote the formation of uniform mesopores, comparing the results so obtained with those corresponding to the use of a non-hierarchical ZSM-5 material as parent sample. Thereby, four ZSM-5 samples were synthesized using different procedures. A non-hierarchical reference sample (ZSM-5) was prepared without including any precrystallization nor silanization step during its synthesis. A second reference ZSM-5 sample, having hierarchical porosity, was synthesized according to the protozeolitic silanization route, being denoted as h-ZSM-5. Both samples were subsequently subjected to the mesopore narrowing treatment leading to the materials named as ZSM-5 (mnt) and h-ZSM-5 (mnt), respectively.

Figure 1 shows the XRD patterns corresponding to the ZSM-5 samples. They display the typical reflections of the MFI structure and no broad bottom reflection in the range $2\theta \sim 20 - 25^\circ$,

proceeding from amorphous material, was appreciated. This fact indicates the highly zeolitic nature of the four ZSM-5 samples, showing that the surfactant/ammonia treatment does not affect their crystallinity. While the intensity of the XRD peaks decreases for the non-hierarchical zeolite after this treatment, the opposite is observed when using the hierarchical ZSM-5 as parent sample.

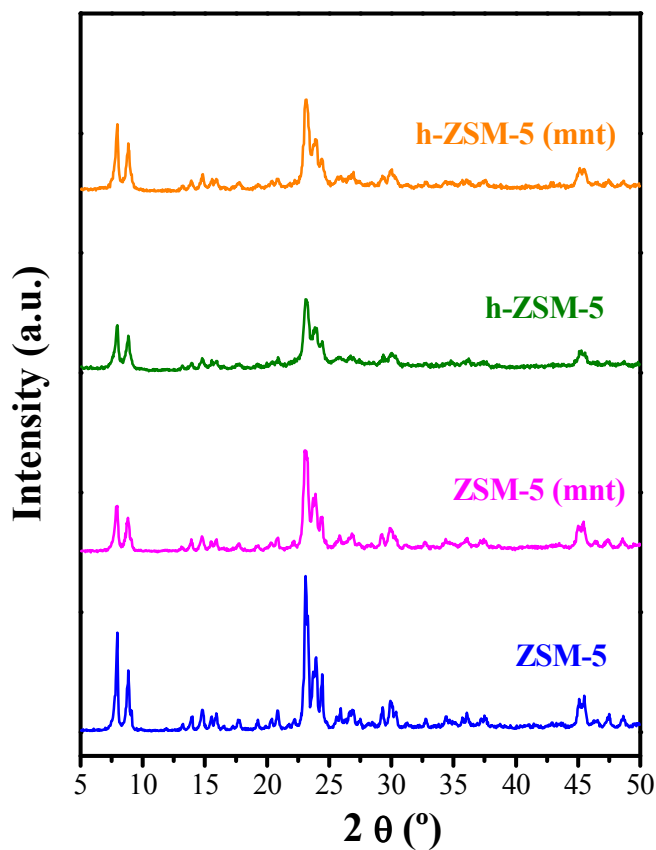


Figure 1. High-angle XRD patterns of the ZSM-5 samples.

These variations suggest that some changes have occurred in the effective size of the crystalline domains after the surfactant/ammonia treatment. For the non-hierarchical ZSM-5, the decrease in the intensity could be indicative of a lower crystallinity, although no amorphous phase is detected in this sample whereas desilication does not seem to be produced, at least

significantly, since the Si/Al ratio remains almost constant (see Table 1). In contrast, for the h-ZSM-5 sample the situation is different since it is made up of aggregates of crystalline nanounits, so it is feasible that the surfactant/ammonia treatment could induce their partial merge, leading towards some growth in the size of the crystalline domains.

Table 1. Physicochemical properties of the ZSM-5 samples.

Sample	Si/Al ^{a)}	SA content ^{b)}	S _{BET} (m ² /g)	S _{ZMP} ^{c)} (m ² /g)	S _{SP+EXT} ^{c)} (m ² /g)	V _{TOT} (cm ³ /g)	V _{ZMP} ^{c)} (cm ³ /g)	V _{SP+EXT} ^{c)} (cm ³ /g)
ZSM-5	28	0.0	420	344	76	0.403	0.198	0.205
ZSM-5 (mnt)	27	0.0	395	276	119	0.447	0.159	0.288
h-ZSM-5	30	0.08	562	259	303	0.504	0.149	0.355
h-ZSM-5 (mnt)	32	0.08	464	262	202	0.483	0.151	0.332

^{a)} Calculated by ICP-AES; ^{b)} Ratio silicon from silanization agent PHAPTMS / total silicon; ^{c)} ZMP: zeolite micropores; SP+EXT: secondary+external porosity.

The yields of solids attained after the surfactant/ammonia treatment was in both cases over 85 wt%. Taking into account that in practice is not possible to recover by centrifugation all the zeolitic material due to the small particle size of the samples, this means that the real yields are even higher. In this way, as shown in Table 1, the Si/Al of the samples after the surfactant/ammonia treatment are very similar to those of the parent zeolites. This result suggests that, if any dissolution of the zeolite has occurred during the surfactant/ammonia treatment, it has affected in a very similar extent to both silicon and aluminium atoms, so the overall zeolite Si/Al ratio is little changed. These findings are clear indications that the ZSM-5 zeolite is quite stable against bulk dissolution and desilication when hydrothermally treated with the surfactant/ammonia solution, which can be related with the mild basicity provided by the ammonia solution.

Two main tools have been used to investigate the porosity of the ZSM-5 samples: Ar adsorption-desorption isotherms and TEM measurements. Figure 2 shows the cumulative pore volumes (left side) and the corresponding pore size distributions (PSD) (right side), calculated by

application of the NLDFT model to the adsorption branch of the Ar adsorption isotherms. This model has the advantage of providing a continuous pore size distribution that covers the whole range of micro- and mesopores, hence it is very well suited for being applied to materials with hierarchical porosity.

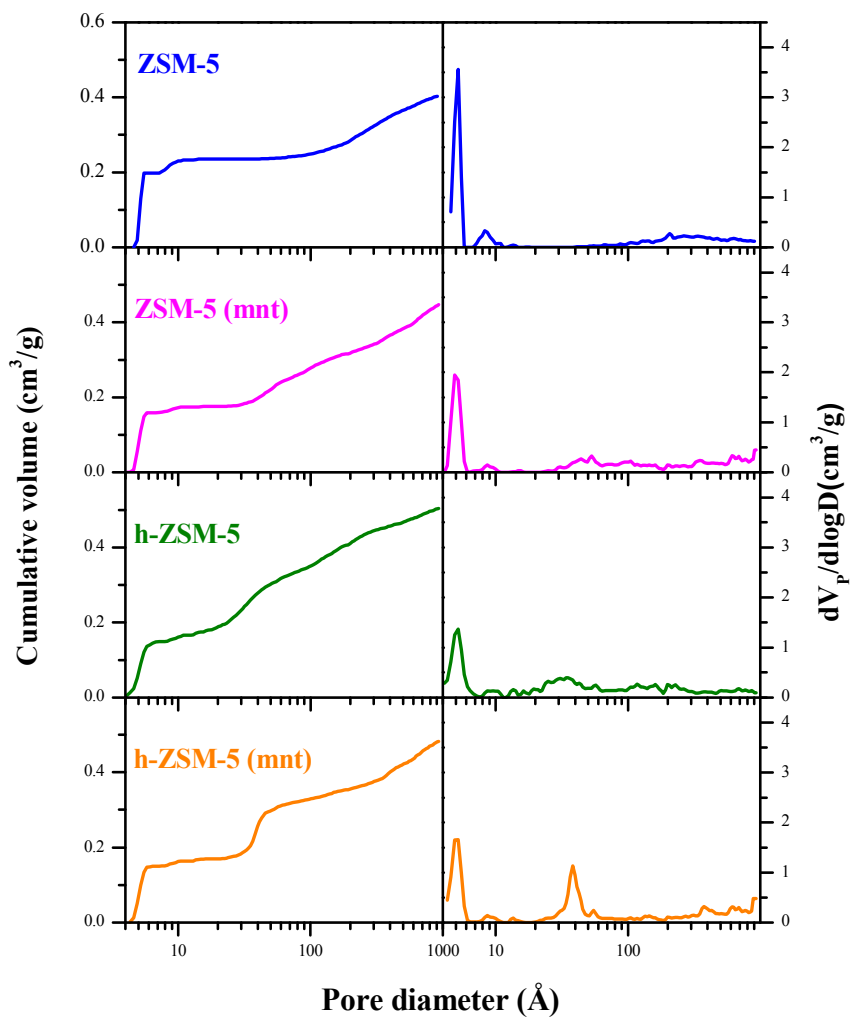


Figure 2. Ar adsorption-desorption isotherms at 87.5 K of the ZSM-5 samples: a) cumulative pore volumes and b) pore size distributions, determined by application of the NLDFT model.

For the parent ZSM-5 sample just a main peak is observed in the PSD at about 0.56 nm, which matches well with the zeolitic micropores. It should be mentioned that a small step is appreciated around 0.8 - 1 nm in the cumulative pore volume curve, which corresponds to the peak, located in the same range, in the pore size distribution. This step has been attributed in the literature to a fluid-to-crystalline transition of the Ar adsorbed in the MFI micropores³⁶ or to crystalline phase transitions³⁷, hence being not associated to any real porosity. The adsorption observed in the parent ZSM-5 sample for pores larger than 20 nm is really originated by the external surface area and intercrystalline voids, as this material is formed by nanocrystals with sizes in the range 20 – 80 nm (see TEM images in Figure 3). When this sample is subjected to the surfactant/ammonia treatment, the material so obtained (ZSM-5 (mnt)) exhibits lower microporosity, whereas a very broad mesopore distribution appears within the 3 – 20 nm range. This result indicates that in this case the surfactant/ammonia treatment is capable of generating some mesoporosity but with little pore size uniformity.

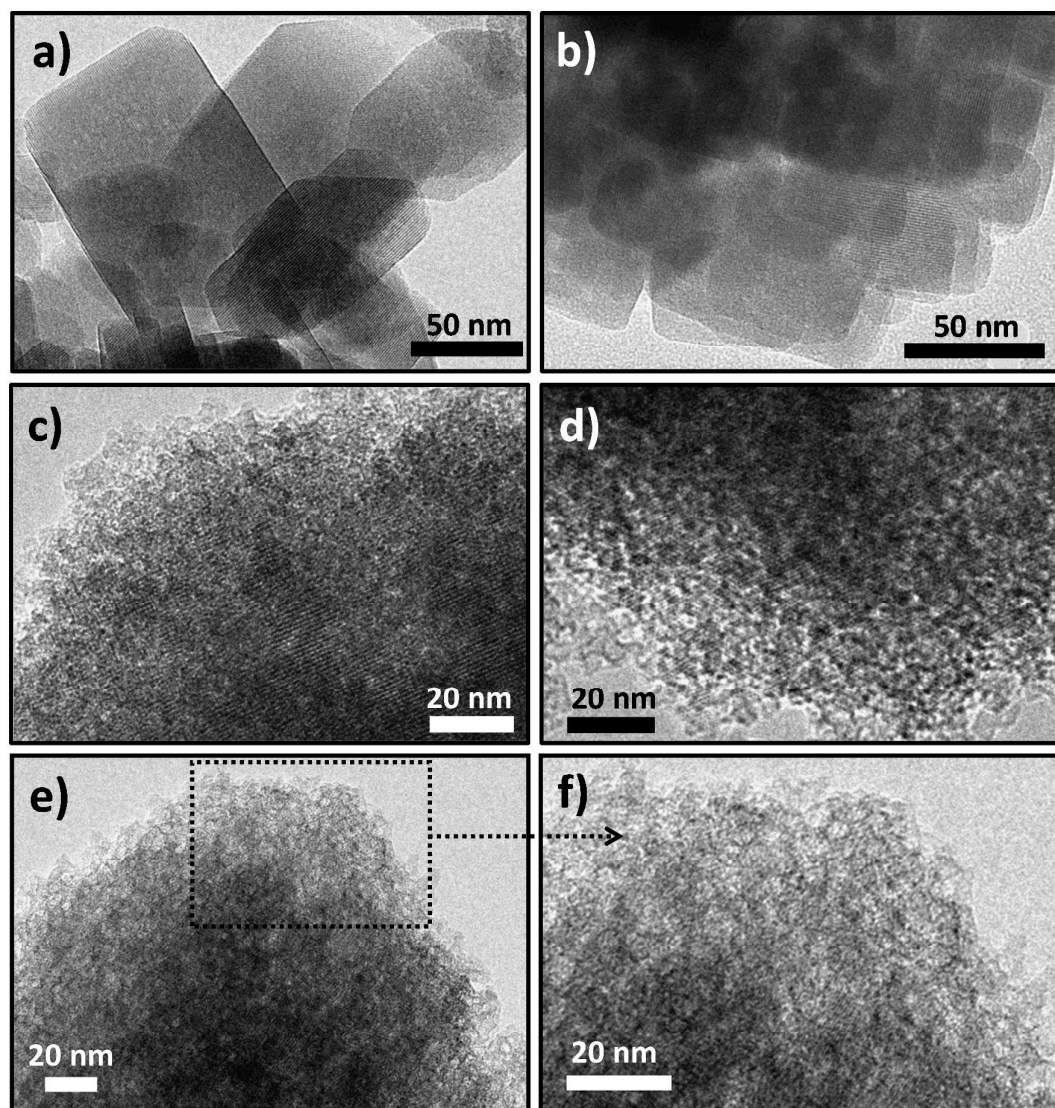


Figure 3. TEM micrographs of the ZSM-5 samples: a) ZSM-5, b) ZSM-5 (mnt), c) h-ZSM-5 and d), e) and f) h-ZSM-5 (mnt).

For the h-ZSM-5 sample, prepared from silanized protozeolitic units, the presence of a hierarchical porosity with at least two levels of pore sizes is evidenced. The secondary porosity in this parent material possesses a broad size distribution mainly within the 2 - 10 nm range, whereas the adsorption occurring at larger pore sizes is really associated to the external surface area located in the outer part of the zeolite particles. However, this picture drastically changes

after the surfactant/ammonia treatment. Thus, for the h-ZSM-5 (mnt) sample, two well-defined adsorption steps are observed in the cumulative pore volume curve, corresponding to micro- and mesopores, respectively. This is confirmed by the pore size distribution of this material as it presents two narrow peaks: the zeolitic micropore peak at about 0.56 nm and a second one centered at ca. 4 nm. From these results, it can be concluded that the surfactant/ammonia treatment is very effective in modifying the mesoporosity existing in the parent hierarchical ZSM-5, narrowing its pore size distribution and leading to the appearance of uniform mesopores. It is particularly noteworthy that this uniform mesoporosity is mainly formed at the expense of the irregular secondary porosity placed within the 2 - 10 nm range.

The main textural properties of the ZSM-5 samples were derived also from the Ar adsorption isotherms at 87 K, being summarized in Table 1. Seemingly, the mesopore narrowing treatment decreases the BET surface values with regard to the reference parent samples. This effect is more pronounced when using the hierarchical zeolite as raw material. The surface area and pore volume associated to the micropores are preserved in the h-ZSM-5 (mnt) sample compared to the parent one, while a significant reduction in these parameters is observed in the case of the non-hierarchical zeolite. Likewise, opposite trends between both types of samples are denoted regarding the secondary porosity. In the case of the hierarchical ZSM-5, the surfactant/ammonia treatment causes a significant decrease of the secondary surface area, which indicates that the new uniform mesopores are mainly formed by reorganization of those previously existing in the parent zeolite. Nevertheless, even after this reduction, the contribution of the secondary surface area in this material (h-ZSM-5 (mnt)) is quite higher than that in the case of the sample prepared from the non-hierarchical ZSM-5 (ZSM-5 (mnt)). The decrease in the micropore volume for the latter after the surfactant/ammonia treatment is accompanied by some enhancement of the external surface area. This is probably due to the surfactant causing some changes in the micropore openings from the outer part of the zeolite crystals as its large

size strongly hinders its penetration into the zeolite micropores. This fact implies that for this material the formation of mesopores occurs from the outer surface of the zeolite crystals inwards and with little possibility of being highly interconnected. However, the mesopore narrowing treatment is not expected to alter the connectivity of the mesopores originally present in the hierarchical ZSM-5 sample.

Figure 3 illustrates TEM micrographs of the ZSM-5 materials. The ZSM-5 sample is made up of cubic-like crystals with a size within the 20 – 80 nm range, hence it can be considered a typical nanocrystalline ZSM-5 sample (Figure 3.a). After the surfactant/ammonia treatment, the aspect of the crystals does not change significantly, and the presence of mesopores is not evident (Figure 3.b). As shown in Figures 3.c, h-ZSM-5 consists of globular shape aggregates formed by very small zeolite nanounits (5 – 10 nm size). The voids existing between these nanounits are irregular and correspond with the secondary porosity identified in this sample from the Ar adsorption-desorption measurements. After the surfactant/ammonia treatment (Figures 3.d, e and f), the similar globular shape aggregates of nanounits are appreciated for the h-ZSM-5 (mnt) sample. However, in this case, the voids existing within the aggregates are more regular in both size and shape, which is in good agreement with the uniform mesopore size distribution obtained from the Ar adsorption-desorption isotherms.

ZSM-5 zeolite is conventionally employed as an acid catalyst due to the presence of acid sites originated from the Al species. Accordingly, the coordination and environment of the Al atoms is an important aspect influencing strongly its catalytic properties. In this way, the ^{27}Al MAS NMR spectra of the ZSM-5 samples after calcination at 550 °C are illustrated in Figure 4. The relative shares of tetrahedral and octahedral aluminium have been approximated by their respective peak area proportion in the ^{27}Al MAS NMR. This procedure is a better choice than the conventional method based on the direct estimation of the peak intensity shares³⁸, since it allows correcting to some extent the effect of strong quadrupolar line broadening leading to invisible

aluminium. ZSM-5 contains mostly tetrahedral aluminium (peak at about 50 ppm, $\text{Al}^{\text{IV}} = 91\%$), incorporated to the zeolite lattice, whereas the proportion of extraframework aluminium is rather low (peak at ca. 0 ppm, $\text{Al}^{\text{VI}} = 9\%$). After the surfactant/ammonia treatment, the relative shares of these two types of Al species for ZSM-5 (mnt) remain almost identical with values about 90 and 10%, respectively. Likewise, the values of the full width at half maximum (FWHM) of the tetrahedral Al peak do not reveal any increase proceeding from the occurrence of distorted aluminium environments, since they were fairly similar for both ZSM-5 (7.1 ppm) and ZSM-5 (mnt) (7.3 ppm) materials. These results confirm that, when using the parent ZSM-5 sample, the zeolite structure is little affected by the combined actions of surfactant and ammonia.

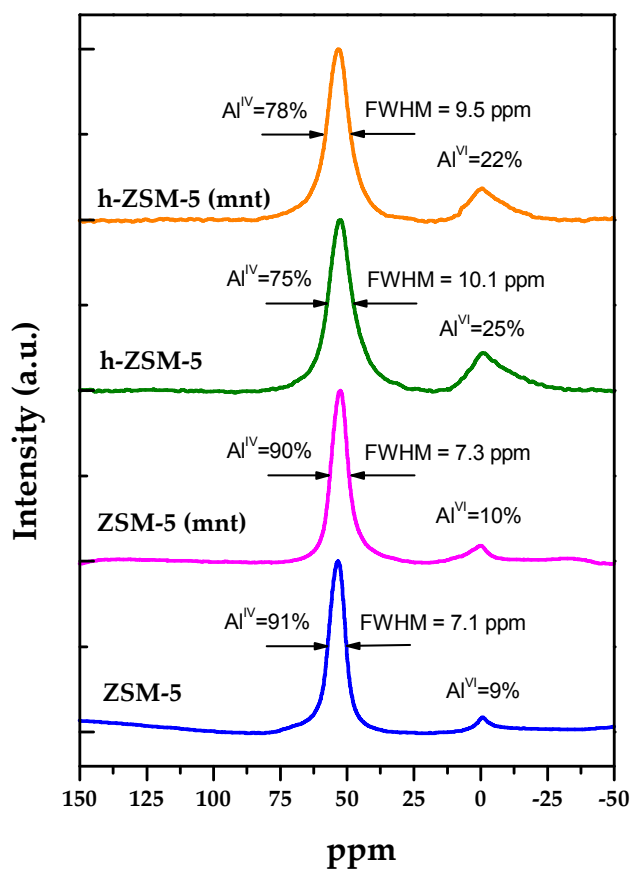


Figure 4. ^{27}Al MAS NMR spectra of the calcined ZSM-5 samples.

On the other hand, it is observed that the parent hierarchical sample (h-ZSM-5) presents a higher contribution of octahedral species and a larger FWHM value compared to ZSM-5. These results agree with previous works and are a result of the remarkable contribution of the secondary porosity in the hierarchical zeolite, which provokes a lower stability and a larger variation of environments of the Al species. In particular, the lower connectivity of the aluminium species located over the secondary porosity of the zeolite causes a higher flexibility in terms of bond angles and lengths^{39,40}. Interestingly, after the surfactant/ammonia treatment, the h-ZSM-5 (mnt) sample exhibits slightly higher proportion of tetrahedral aluminium species than the parent h-ZSM-5, suggesting that a small amount of the extraframework Al species are reincorporated into the zeolite structure, probably by healing some defect sites, such as silanol nests. It is also noteworthy that the value of the FWHM parameter measured for the h-ZSM-5 (mnt) sample (9.5 ppm) is lower than that obtained for h-ZSM-5 (10.1 ppm). This result denotes that the mesopore narrowing treatment here applied increases the uniformity of the aluminium environment in the hierarchical zeolite. Other important aspect to be considered is whether the acid features of the zeolite change after the surfactant/ammonia treatment. In this regard, FTIR measurements of h-ZSM-5 and h-ZSM-5 (mnt) samples after pyridine adsorption were performed at several evacuation temperatures (250, 350 and 450 °C) in order to determine the concentration of both Brönsted (band at 1545 cm⁻¹) and Lewis acid sites (band at 1455 cm⁻¹).

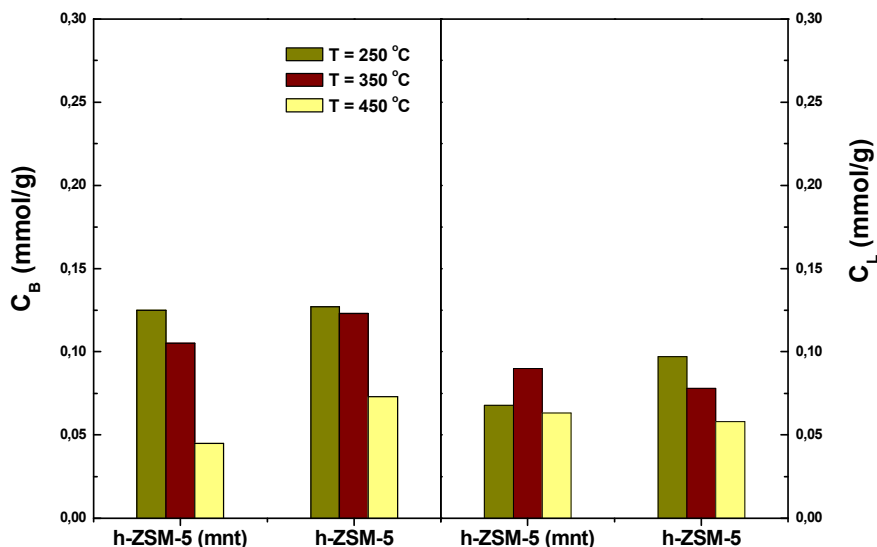


Figure 5. Concentration of Brønsted and Lewis acid sites on h-ZSM-5 (mnt) and h-ZSM-5 samples.

As it can be appreciated in Figure 5, h-ZSM-5 contains a higher concentration of Brønsted acid sites than Lewis ones, as it was expected for this zeolite structure possessing a relatively high Si/Al ratio. Increasing the evacuation temperature provokes a reduction in the amount of both types of acid sites being detected due to the progressive desorption of pyridine molecules, which in turn depends on the strength of the acid sites. Comparing both materials, h-ZSM-5 and ZSM-5 (mnt), no significant variations are detected in the amount and the distribution of Brønsted and Lewis acid sites. These results show that the surfactant-assisted reorganization of the mesoporosity takes place preserving the acid properties of the zeolite. Moreover, this finding is another indication that no amorphous phases are formed during the surfactant/ammonia treatment since, in that case, the ratio of Brønsted/Lewis acid sites should have decreased significantly according to the acidic features which are predominant in amorphous aluminosilicates.

3.2. Synthesis mechanism of hierarchical ZSM-5 zeolite with uniform mesopores

Based on the results above discussed, the scheme shown in Figure 6 is proposed for summarizing the mechanism of the synthesis of hierarchical zeolites with uniform mesoporosity following the approach here reported.

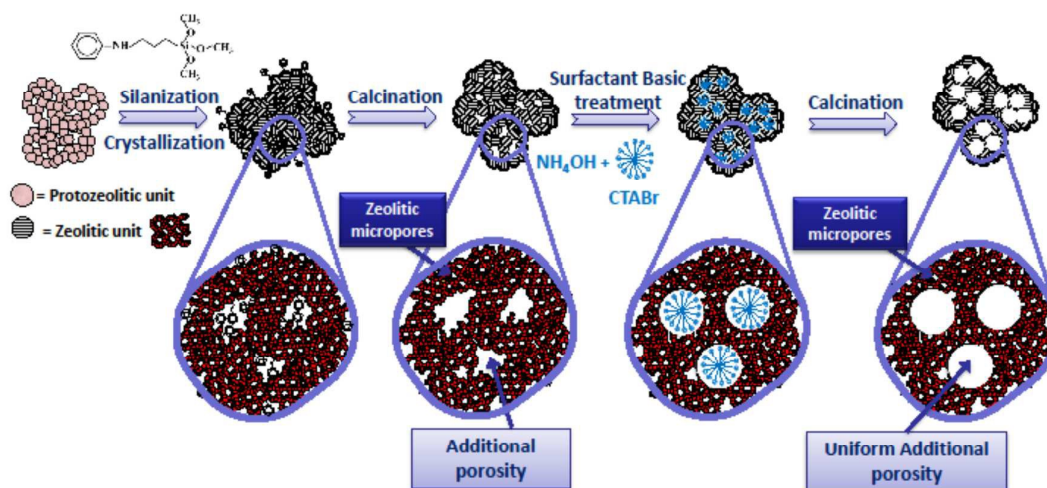


Figure 6. Mechanism of the synthesis of hierarchical ZSM-5 zeolite with uniform mesoporosity.

The first step involves the preparation of a parent zeolite having hierarchical porosity by means of the use of a silanization agent, which is anchored to the external surface of protozeolitic nanounits. Accordingly, during the subsequent hydrothermal treatment, the growth of the silanized protozeolitic nanounits is partially hindered leading to materials that contain, in addition to the structure-directing agent, significant amounts of the silanization reagent. The secondary porosity is generated once the organics have been removed by calcination, although the materials so obtained possess a broad mesopore size distribution. Incorporation of silanization

agents in the range 5 - 8 mol%, regarding the total silica content, is enough for leading to zeolites with a high contribution of the secondary porosity to the overall textural properties.

In a second step, the hierarchical porosity is reorganized by hydrothermal treatment with a surfactant/ammonia solution. The conditions of this treatment are conveniently selected to avoid any damage to the zeolite, such as desilication, dealumination or amorphization. For those employed in the present work, the Si/Al ratio of the zeolite framework remains almost unchanged, hence it can be assumed that desilication does not take place in a significant extension. Likewise, no amorphous phases are formed during the MNT treatment as concluded from the XRD patterns. In fact, the XRD peak intensity of the hierarchical ZSM-5 is increased after being contacted with the surfactant/ammonia solution, which is indicative of some partial merge and growth of the nanounits.

The main changes induced by the mesopore narrowing treatment are observed regarding the textural properties. It is here proposed that the changes undergone by the mesopores occurs mainly according to an Ostwald ripening mechanism, wherein the irregular surface of the secondary porosity is converted into one with more uniformity and less roughness due to the combined effect of the basic conditions and the surfactant. The treatment causes first the breaking of some Si-O-Si or Si-O-Al bonds in the zeolite, partially releasing zeolitic fragments, which are subsequently reorganized by the surfactant over the mesopore surface. Since mild basic conditions are employed, these fragments keep their zeolitic nature, whereas overall dissolution or desilication phenomena are avoided. Subsequently, reconstruction of Si-O-Si or Si-O-Al bonds allows the zeolitic fragments to be linked again to the zeolite nanocrystals. Accordingly, the major role of the surfactant is to rearrange the zeolitic fragments over the mesopore surface. These phenomena affect mainly to the secondary pores with sizes in the range 2 – 10 nm, being transformed into mesopores with diameter about 4 nm. The mesoporosity rearrangement is accompanied by changes in the textural properties, with a decrease of both the

BET and secondary surface areas. Likewise, a more regular environment of the Al species is achieved, as inferred from ^{27}Al MAS NMR measurements.

Interestingly, the surfactant/ammonia treatment is little effective when using as parent zeolite a material free of secondary porosity. Although some changes have been observed in the properties of the zeolite in this case, they are quite less significant and do not lead to a uniform mesoporosity. This can be easily understood as for purely microporous zeolite samples the interaction of the surfactant molecules occurs mainly over the external surface of the crystals, while their access to the internal microporosity is strongly hindered.

3.3. Changes induced in the zeolite catalytic properties

The presence of uniform mesoporosity in hierarchical ZSM-5 is expected to have deep catalytic implications, both in terms of activity and selectivity. These effects should be especially remarkable in those reactions involving bulky compounds and having, consequently, strong diffusional and/or steric limitations for being catalysed by the active sites located within the micropores of conventional zeolites. As it has been demonstrated above, the synthesis strategy here reported allows the secondary porosity present in hierarchical zeolites to be modified, leading to a narrow mesopore distribution. However, this change takes place at the expense of a reduction in the contribution of the secondary porosity, with a decrease in the corresponding surface area and pore volume. Accordingly, an important aspect to be clarified is how these modifications in the share and features of the secondary porosity are going to affect the catalytic behaviour of the hierarchical zeolites. In order to answer these questions, the different zeolite samples were tested in this work as catalysts for the acylation of the bulky reagent 2-methoxynaphthalene. This type of reaction was selected since in previous works it has been found to be very sensitive to the presence of hierarchical porosity in zeolites^{39,40}.

The desired product in the acylation of 2-methoxynaphthalene (2-MN) is 6-acetyl-2-methoxynaphthalene (6A-2MN), which is an intermediate for the manufacture of the anti-inflammatory drug Naproxen. As shown in scheme 1, direct acylation reactions (A) results in the formation of both 1-acetyl-2-methoxynaphthalene (1A-2MN) and the desired 6A-2MN⁴¹. However, the 1 position of 2-methoxynaphthalene is the most active, being kinetically favoured, so 1A-2MN is the major product initially formed. As the reaction proceeds, the desired isomer 6A-2MN, thermodynamically most stable, is also produced by intermolecular transacylation reactions (T) involving both 2-MN and 1A-2MN^{42,43}. Additionally, 8-acetyl-2-methoxynaphthalene (8A-2MN) may be generated by means of intramolecular transacylation reactions of the 1A-2MN isomer.

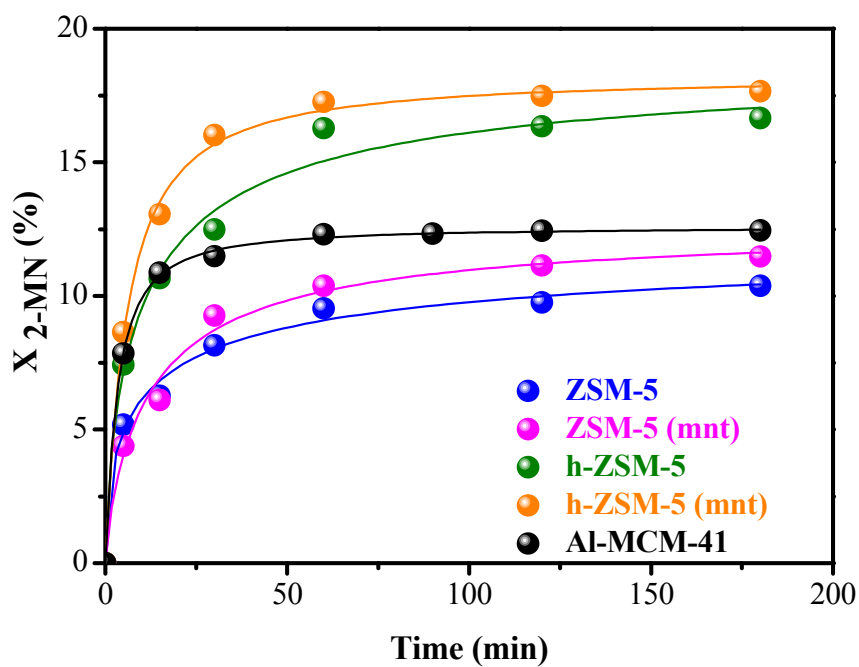
Figure 7 illustrates the evolution of the 2-methoxynaphthalene conversion and the 6A-2MN selectivity along the time obtained over the different zeolite samples here investigated. For comparison, an Al-MCM-41 sample has been included in the catalytic tests in order to determine the behaviour of an amorphous aluminosilicate with ordered mesoporosity. This sample shows a high BET surface area ($893 \text{ m}^2 \text{ g}^{-1}$) consisting of uniform mesopores of 2.7 nm without any microporosity, hence its performance as catalyst in reactions involving bulky molecules is not limited by steric or diffusional factors as it usually occurs with conventional zeolites having just micropores. Additionally, the Al-MCM-41 Si/Al atomic ratio (28) is very close to that of the ZSM-5 catalysts used in this work, although containing mostly Lewis acid sites of medium strength. Therefore, this Al-MCM-41 sample is a convenient reference material to compare its catalytic performance with those of the ZSM-5 samples here investigated and to assess the effects that could be derived from the presence of any ordered mesophase after the surfactant/ammonia mesopore narrowing treatment.

The reactions have been performed at 180 °C using acetyl chloride as acylating agent. In all cases, the conversion evolves increasing with time until a plateau is reached after 60 min of reaction. This can be indicative of a catalyst deactivation or, as reported for other acylation

reactions, to a product inhibition effect caused by the strong adsorption of the reaction products on the active sites⁴⁴. Comparing the two parent zeolite samples, it is evident that the hierarchical ZSM-5 presents a quite superior catalytic activity. Thus, the conventional ZSM-5 sample showed the poorest activity because of its inferior textural properties as it possesses the lowest external/mesopore surface area ($S_{\text{ext+SP}} = 76 \text{ m}^2\text{g}^{-1}$). This fact originates that conventional ZSM-5 experiences strong steric hindrances for the acylation of the bulky 2-MN, exhibiting quite lower conversion compared to the hierarchical ZSM-5 sample.

After the surfactant/ammonia treatment a significant enhancement of the conversion for both materials is observed, the highest one corresponding again to that obtained from the hierarchical zeolite. Thus, the improvement of the conversion for h-ZSM-5 (mnt) is more pronounced, in particular at short reaction times when the product inhibition effect is less significant. Therefore, in this case the presence of uniform mesoporosity has an important positive effect on the catalytic activity. It is also noteworthy that the Al-MCM-41 sample shows worse results than the two hierarchical ZSM-5 zeolites, reaching a plateau for a 2-MN conversion about 12%. Taking into account the superior textural properties of Al-MCM-41 (very high surface area and uniform mesopores), the cause of the lower activity observed for this sample compared to the two hierarchical ZSM-5 materials is to be ascribed to the occurrence of acid sites of lower acid strength than those present over both zeolitic catalysts. This result is relevant as it confirms the absence of amorphous ordered mesoporous phases in the h-ZSM-5 (mnt) sample since, in that case, the 2-MN conversion obtained with the latter should have been lower than that of hierarchical ZSM-5.

a)



b)

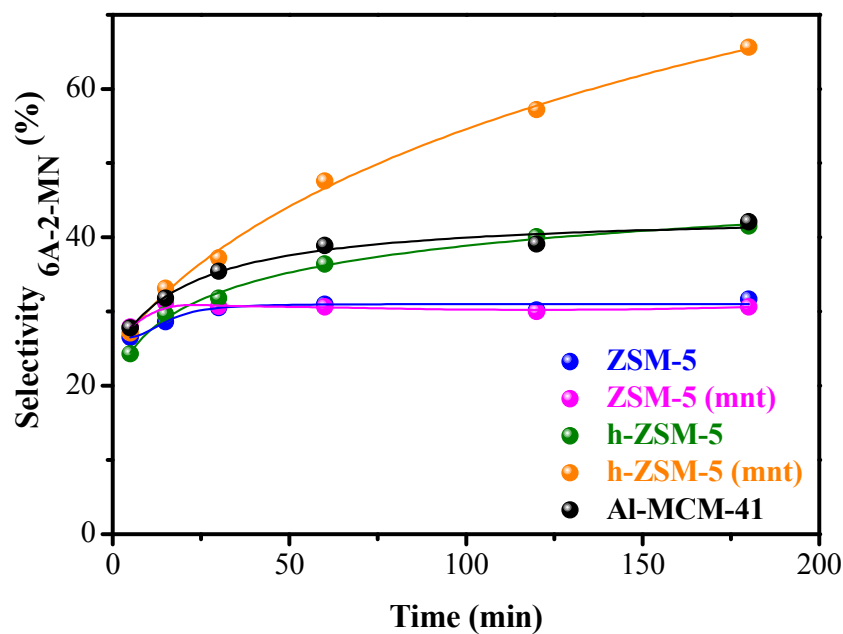


Figure 7. Acylation of 2-methoxynaphthalene. Evolution along the reaction time of: a) 2-MN conversion and b) 6A-2MN selectivity.

On the other hand, significant differences are observed between the samples when compared in terms of selectivity towards the desired product. The reference h-ZSM-5 shows higher selectivity towards 6A-2MN compared to the conventional sample (ZSM-5) and Al-MCM-41. In the case of Al-MCM-41, it has been reported that the selectivity obtained in the 2-MN acylation is addressed mainly to the production of 1A-2MN because of the unrestrained nature of its mesopores^{45,46}. Interestingly, for the hierarchical ZSM-5 sample the 6A-2MN selectivity is further improved after the mesopore narrowing treatment, increasing continuously along the reaction time (Figure 7.b). As a result, the selectivity obtained over the h-ZSM-5 (mnt) sample is very superior to that of the other catalysts. Thus, h-ZSM-5 (mnt) allowed obtaining 65.8% selectivity towards 6A-2MN after 3 h of reaction, quite higher than that of the next catalyst (h-ZSM-5, 41.5% selectivity). It is noteworthy that this enhancement in selectivity occurs despite the above commented loss of secondary surface area after the surfactant/ammonia treatment, so its origin must be related to the uniformity of the attained mesoporosity. These results denote that a more uniform mesoporosity enhances the activity of both the acylation and the intermolecular transacylation reactions, resulting in an increase of the substrate conversion simultaneously with a quite superior selectivity (over 60% at the longest reaction time) towards the target product over the h-ZSM-5 (mnt) sample. Interestingly, the 6A-2MN selectivity value here obtained is quite similar to the best ones so far published corresponding to Beta zeolite, that has been regarded as the benchmark catalyst for this reaction due to the shape selectivity effect of its 3D 12 membered ring channels⁴⁷⁻⁴⁹. Thus, when comparing Beta, USY, SSZ-33, SSZ-35 and ITQ-32 zeolites in the acylation of 2-methoxynaphthalene with acetic anhydride⁵⁰, Beta zeolite gave rise to the highest selectivity towards 6A-2MN with values around 60%.

The improved catalytic properties observed after the surfactant/ammonia treatment are ascribed mainly to the enhanced homogeneity of the mesopore features (size, geometry and

surface). The presence of uniform mesopores involves an enhanced mass transfer of the reagent molecules through channels with a lower tortuosity factor. On the other hand, a smooth uniform mesopore surface is more amenable to adsorption of the reacting molecules than a rough one, being less affected by steric limitations that could hinder the contact between bulky compounds and some of the active sites located over the mesopore surface. In other words, a more uniform mesoporosity increases the catalytic effectiveness of the mesopore surface area, since it favours the participation in the reaction of all the active sites there located, giving rise to higher intrinsic activities.

4. CONCLUSIONS

Hierarchical ZSM-5 zeolite with uniform mesopore size distribution has been successfully prepared by the combination of two approaches: crystallization of silanized protozeolitic units to generate a secondary porosity and surfactant/ammonia-mediated reorganization of the latter. The application of the mesopore narrowing treatment to hierarchical ZSM-5 allowed the previously existing irregular secondary porosity (about 2 – 10 nm range) to be transformed into uniform mesopores with sizes centered at 4 nm. In contrast, the surfactant/ammonia treatment had little effect when applied to a zeolite sample free of the initial secondary porosity.

It is proposed that the uniform mesoporosity is generated by means of the local rearrangement of zeolitic fragments according to an Ostwald ripening mechanism, wherein the irregular surface of the secondary porosity is converted into one quite more uniform and with less roughness due to the combined effect of the mild basic conditions and the surfactant. This picture is consistent with the absence of amorphous phases and the negligible variations produced in the zeolite framework composition after the mesopore narrowing treatment, showing the stability of the ZSM-5 structure against amorphization and desilication phenomena, probably due to the mild basicity of the ammonia solution. The presence of a more regular mesoporosity in hierarchical

ZSM-5 is accompanied by a higher uniformity of the Al sites environment, whereas the zeolite acid properties are preserved without any significant variation.

The effects of having uniform mesopores on the catalytic behaviour have been proved in the acylation of 2-methoxynaphthalene. Higher activity, as well as superior selectivity towards the desired 6-acetyl-2-methoxynaphthalene isomer, was obtained over the hierarchical ZSM-5 with uniform mesopores. These effects are consequences of the enhanced homogeneity of both the mesopore features (size, geometry and surface) and the environment of the corresponding active sites, which in turn lead to an improved catalytic behaviour.

6. ACKNOWLEDGMENTS

The authors want to thank the funding by the Spanish government through the projects ENE2011 – 29643 – C02 – 01 and CTQ 2011/22707. We want to thank Dr. J. L. García Fierro from ICP-CSIC for performing the pyridine adsorption measurements shown in this work.

7. REFERENCES

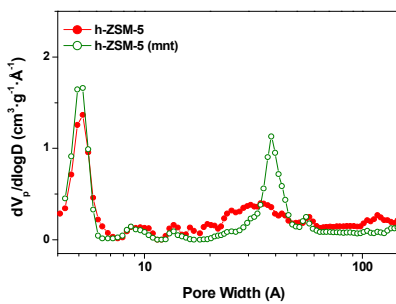
1. D. P. Serrano, J. M. Escola, P. Pizarro, *Chem. Soc. Rev.* 2013, **42**, 4004.
2. D. P. Serrano, J. Aguado, J.M. Escola, *Catalysis*, 2011, **23**, 253.
3. J. Pérez-Ramírez, C. H. Christensen, K. Egeblad, C. H. Christensen, J. C. Groen, *Chem. Soc. Rev.* 2008, **37**, 2530.
4. K. Egeblad, C. H. Christensen, M. Kustova, C. H. Christensen, *Chem. Mater.* 2008, **20**, 946.
5. J. Cejka, G. Centi, J. Pérez-Pariente, W. J. Roth, *Catal. Today* 2012, **179**, 2.
6. H. Wang, T. J. Pinnavaia, *Angew. Chem. Int. Ed.* 2006, **45**, 7603.
7. M. Choi, H. S. Cho, R. Srivastava, C. Verkatesan, D. H. Choi, R. Ryoo, *Nat. Mater.* 2006, **5**, 718.

8. K. Na, C. Jo, J. Kim, K. Cho, J. Jeng, Y. Seo, R. J. Messinger, B. F. Chmelka, R. Ryoo, *Science* 2011, **333**, 328.
9. D. P. Serrano, J. Aguado, J. M. Escola, J. M. Rodriguez, A. Peral, *Chem. Mater.* 2006, **18**, 2462.
10. D. P. Serrano, J. Aguado, G. Morales, J. M. Rodriguez, A. Peral, M. Thommes, J. D. Epping, B. F. Chmelka, *Chem. Mater.* 2009, **21**, 641.
11. C. H. J. Jacobsen, C. Madsen, J. Houzvicka, I. Schmidt, A. Carlsson, *J. Am. Chem. Soc.* 2000, **122**, 7116.
12. C. H. Christensen, K. Johansson, E. Törnqvist, I. Schmidt, H. Topsøe, C. H. Christensen, *Catal. Today* 2007, **128**, 117.
13. D. H. Park, S. S. Kim, H. Wang, T. J. Pinnavaia, M. C. Papapetrou, A. A. Lappas, K. S. Triantafyllidis, *Angew. Chem. Int. Ed.* 2009, **48**, 7645.
14. J. M. Escola, J. Aguado, D. P. Serrano, A. García, A. Peral, L. Briones, R. Calvo, E. Fernández, *Appl. Catal. B* 2011, **106**, 405.
15. A. Grau-Atiienza, R. Campos, E. Serrano, M. Ojeda, A.A. Romero, J. García-Martínez, R. Luque, *ChemCatChem*. 2015, **6**, 3530.
16. R. Srivastava, M. Choi, R. Ryoo, *Chem. Commun.* 2006, 4489.
17. G. T. Kerr, *J. Phys. Chem.* 1967, **71**, 4155.
18. J. C. Groen, J. C. Jansen, J. A. Moulijn, J. Pérez-Ramírez, *J. Phys. Chem. B* 2004, **108**, 13062.
19. M. Millina, S. Mitchell, P. Crivelli, D. Cooke, J. Pérez-Ramírez, *Nature Commun.* 2014, **5**, 3922.
20. M. Millina, S. Mitchell, D. Cooke, P. Crivelli, J. Pérez-Ramírez, *Angew. Chem. Int. Ed.* 2015, **54**, 1591.

21. J. C. Kim, R. Ryoo, M. V. Opanasenko, M. V. Shamzy, J. Cejka, *ACS Catalysis* 2015, **5**, 2596.
22. R. Srivastava, N. Iwasa, S. Fujita, M. Arai, *Chem. Eur. J.* 2008, **14**, 9507.
23. Z. Xue, T. Zhang, J. Ma, H. Miao, W. Fan, Y. Zhang, R. Li, *Micropor. Mesopor. Mater.* 2012, **151**, 271.
24. D. P. Serrano, J. Aguado, J. M. Escola, J. M. Rodríguez, A. Peral, *J. Mater. Chem.* 2008, **18**, 4210.
25. D. P. Serrano, J. Aguado, J. M. Escola, A. Peral, G. Morales, E. Abella, *Catal. Today* 2011, **168**, 86.
26. V. N. Shetti, J. Kim, R. Srivastava, M. Choi, R. Ryoo, *J. Catal.* 2008, **254**, 296.
27. A. J. J. Koekkoek, C. H. L. Tempelman, V. Degirmenci, M. Guo, Z. Feng, C. Li, E. J. M. Hensen, *Catal. Today* 2011, 168, 96.
28. A. Bonilla, D. Bauduin, J. Pérez-Ramírez, *J. Catal.* 2009, **265**, 170.
29. S. Abelló, A. Bonilla, J. Pérez-Ramírez, *Appl. Cat. A* 2009, **364**, 191.
30. K. P. De Jong, J. Zecevic, H. Friedrich, P. E. De Jong, M. Bulut, S. Van Donk, K. Keumogne, A. Finiels, V. Hulea, F. Fajula, *Angew. Chem. Int. Ed.* 2010, **49**, 10074.
31. J. Y. Ying, J. García-Martínez, *US Patent* 2009; 7,589,041.
32. R. Chal, T. Cacciaguerra, S. Van Donk, C. Gerardin, *Chem. Commun.* 2010, **46**, 7840.
33. D. P. Serrano, R. Sanz, P. Pizarro, I. Moreno, S. Shami, *Micropor. Mesopor. Mater.* 2014, **189**, 71.
34. A. Matsumoto, H. Chen, K. Tsusumi, M. Grün, K. Unger, *Micropor. Mesopor. Mater.* 1999, **32**, 55.
35. C. A. Emeis, *J. Catal.* 1993, **141**, 347.
36. J. C. Groen, L. A. Peffer, J. Pérez-Ramírez, *Microporous Mesoporous Mater.* 2003, **60**, 1.
37. K. Nakai, J. Sonoda, M. Yoshida, M. Hakuman, H. Naono, *Adsorption* 2007, **13**, 351.

38. G. Engelhardt, *Stud. Surf. Sci. Catal.* 2001, **137**, 387.
39. D. P. Serrano, R. A. García, G. Vicente, M. Linares, D. Procházková, J. Cejka, *J. Catal.* 2011, **279**, 366.
40. D. P. Serrano, R. A. Garcia, M. Linares, B. Gil, *Catal. Today* 2012, **179**, 91.
41. G. Sartori, R. Maggi, *Chem. Rev.* 2006, **106**, 1077.
42. M. Selvaraj, K. Lee, K. S. Yoo, T. G. Lee, *Microporous Mesoporous Mater.* 2005, **81**, 343.
43. E. Fromentin, J. M. Coustard, M. Guisnet, *J. Catal.* 2000, **190**, 433.
44. J. M. Escola, M. E. Davis, *Appl. Catal. A* 2001, **214**, 111.
45. E. A. Gunnewegh, S. S. Gopie, H. van Bekkum, *J. Mol. Cat. A*, 1996, **106**, 151.
46. B. Lindlar, A. Kogelbauer, R. Prins, *Micropor. Mesopor. Mater.* 2000, **38**, 167.
47. X. Ouyang, S. J. Hwang, R. C. Runnebaum, D. Xie, Y. J. Wanglee, T. Rea, S. I. Zones, A. Katz, *J. Am. Chem. Soc.* 2014, 136, 1449.
48. P. Andy, J. García-Martínez, G. lee, H. González, C. Jones, M. E. Davis, *J. Catal.* 2000, 192, 215 – 223.
49. G. Harvey, G. Mader, *Collect. Czech., Chem. Commun.* 1992, 57, 862.
50. D. Vitvarova, L. Lupinkova, M. Kubu, *Micropor. Mesopor. Mater.* 2015, 210, 133.

Table of contents



- Uniform mesopores are generated in hierarchical ZSM-5 by the MNT treatment, originating enhanced activity in the acylation of 2-methoxynaphthalene.